Dalton Transactions

Accepted Manuscript

ROYAL SOCIETY OF CHEMISTRY

www.rsc.org/dalton

Synthesis, characterization, and H/D exchange of μ-hydride-containing [FeFe]-hydrogenase subsite models formed by protonation reactions of $(\mu\text{-TDT})Fe_2(CO)_4(PMe_3)_2$ (TDT = SCH_2SCH_2S) with protic acids†

Li-Cheng Song,*[1,2] An-Guo Zhu,[1,2] and Yuan-Qiang Guo[1,2]

As [FeFe]-hydrogenase models, the first thiodithiolate (TDT) ligand-containing μ-hydride complexes $[(\mu\text{-TDT})Fe_2(CO)_4(PMe_3)_2(\mu\text{-H})]^+Y^-$ (**2–7**, Y = Cl, ClO_4, PF_6, BF_4, CF_3CO_2, CF_3SO_3) have been prepared by protonation reactions of $(\mu\text{-TDT})Fe_2(CO)_4(PMe_3)_2$ (**1**) with the corresponding HY acids. While the protonation reactions are monitored by in situ ^1H and $^{31}P\{^1H\}$ NMR spectroscopy to show the isomer type and stability of **2–7**, the structures of the isolated **2–7** are characterized by elemental analysis, spectroscopy and for some of them by X-ray crystallography. Although the H/D exchange of μ-hydride complex **7** (Y = CF_3SO_3) with D_2 or D_2O has been proved not to occur under the studied conditions, the H/D exchange of **7** with DCl gives the μ-deuterium complex $[(\mu\text{-TDT})Fe_2(CO)_4(PMe_3)_2(\mu\text{-D})]^+[CF_3SO_3]^-$ (**8**) in a nearly quantitative yield. To our knowledge, **8** is the first crystallographically

[1]*Department of Chemistry, State Key Laboratory of Elemento-Organic Chemistry,* [2]*Collaborative Innovation Center of Chemical Science and Engineering (Tianjin), Nankai University, Tianjin 300071, China E-mail: lcsong@nankai.edu.cn.*

† Eelectronic supplementary information (ESI) available: selected bond lengths (Å) and angles (°) for **1, 3-5**, and **8** (Tables S1, S2 and S7), crystal data and structural refinements details for **1, 3-5**, and **8** (Tables S8 and S9), in situ ^1H NMR of μ-H in **2-7** and in situ $^{31}P\{^1H\}$ NMR of **2-7** taken after the 5 min protonation reactions of complex **1** with the corresponding acids (Tables S3 and S4, Figs. S1 and S2), in situ ^1H NMR of μ-H in **5** and in situ $^{31}P\{^1H\}$ NMR of **5** taken at time intervals (Tables S5 and S6, Figs. S3 and S4), and discussion of the unsuccessful H/D exchange results. CCDC reference numbers 1427568-1427572. For ESI and crystallographic data in CIF or other electronic format see DOI: 10.1039/b000000x/.

characterized μ-deuterium-containing butterfly [2Fe2S] complex produced by H/D exchange reaction.

Introduction

[FeFe]-hydrogenases ([FeFe]Hases) have received great attention in recent years, largely due to their unique structure and particularly the extremely high catalytic efficiency for proton reduction and hydrogen oxidation in a variety of microorganisms.[1-4] The X-ray crystallographic study on [FeFe]Hases revealed that the active site of [FeFe]Hases contains a butterfly [2Fe2S] catalytic subsite and a cubic [4Fe4S] electron-transfer unit, which are linked together via a cysteine S atom. In addition, the two Fe atoms in the [2Fe2S] subsite are bridged by a dithiolate cofactor and coordinated by the biologically unusual CO and CN^- ligands (Fig. 1).[5-7] Recently, the debate about nature of bridging dithiolate cofactor has been settled by the presented evidences of ^{14}N HYSCORE and controlled metalloenzyme activation in favor of azadithiolate.[8,9]

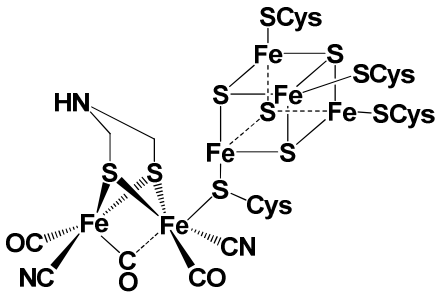

Fig. 1 The active site structure of [FeFe]-hydrogenases.

Inspired by the well-elucidated active site structure shown in Figure 1, synthetic chemists have prepared a wide variety of biomimetic models for the active site of

[FeFe]Hases.[10-29] However, it is worth noting that among the prepared models the μ-hydride-containing PMe_3-disubstituted diiron complexes are of particular interest since they can act as the structural and functional models for the protonated diiron subsite generated during the course of proton reduction or H_2 oxidation catalyzed by [FeFe]Hases.[30-37] To date, although some PMe_3-disubstituted diiron complexes such as (μ-PDT)$Fe_2(CO)_4(PMe_3)_2$, (μ-ODT)$Fe_2(CO)_4(PMe_3)_2$, and (μ-ADT)$Fe_2(CO)_4(PMe_3)_2$, as well as their μ-hydride complexes have been prepared,[30-37] no their TDT analogue (μ-TDT)$Fe_2(CO)_4(PMe_3)_2$ (**1**, TDT = SCH_2SCH_2S) and the corresponding protonated products are reported, so far. To further develop the biomimetic chemistry of [FeFe]Hases and to examine the isomer structures and properties of the μ-hydride complexes generated by protonation reactions of complex **1** with some protic acids, we launched this study. Herein we report the interesting results obtained by this study.

Results and discussion

Synthesis and characterization of PMe_3-disubstituted complex (μ-TDT)$Fe_2(CO)_4(PMe_3)_2$ (1)

Although the parent TDT-type complex (μ-TDT)$Fe_2(CO)_6$ (**A**) and some of its CO substitution derivatives were previously reported,[38,39] the PMe_3-disubstituted derivative of **A**, namely complex **1** has not yet appeared in literature, to date. Similar to preparation of its PDT and ODT analogues,[33,35,36] complex **1** could be prepared by reaction of parent complex **A** with excess PMe_3 in refluxing hexane in 80% yield (Scheme 1).

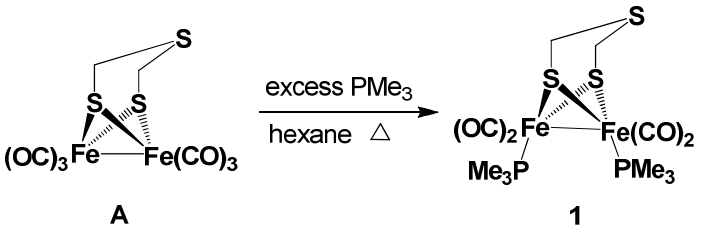

A 1

Scheme 1 Synthesis of complex **1**

Complex **1** is a slightly air-sensitive red solid and has been characterized by elemental analysis and spectroscopy. For example, the IR spectrum of **1** showed three absorption bands in the range 1979–1898 cm^{-1} for its terminal carbonyls. These bands are considerably shifted towards lower energy relative to those (2075–1990 cm^{-1}) of its parent complex **A**. This is apparently due to the increased electron density at the Fe centers by CO substitution with the stronger electron donor PMe_3. The ^1H NMR spectrum of **1** displayed a singlet at 3.22 ppm for its methylene protons and a doublet at 1.56 ppm for its PMe_3 protons. In addition, the $^{31}P\{^1H\}$ NMR spectrum of **1** exhibited a singlet at 22.2 ppm for P atoms in its PMe_3 ligands. In general, complexes of this type may exist as four isomers: ap/ap, ap/ba, cis-ba/ba, and trans-ba/ba isomers (Scheme 2).[40,41]

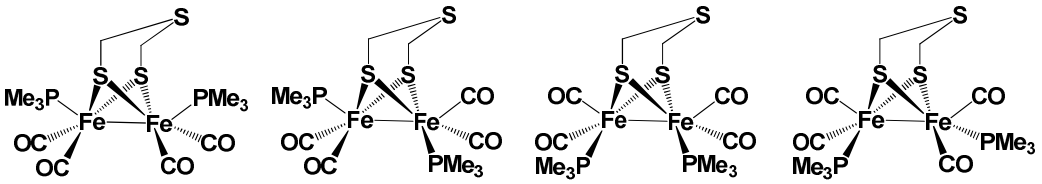

Scheme 2 Four possible isomers of complex **1**

To confirm the isomer structure of **1**, an X-ray crystallographic study was undertaken. While Fig. 2 shows its ORTEP plot, Table S1 lists its selected bond lengths and angles. Interestingly, Fig. 2 shows that complex **1** exists only as one

isomer, namely the trans-ba/ba isomer, in which its two PMe_3 ligands lie in two basal positions of the two square-pyramidal Fe centers with a trans coordination mode. It follows that our complex **1** adopts the same type of solid-state structure as that for its PDT analogue reported by Darensbourg and co-workers,[40] but different from its ODT analogue that adopts the ap/ba type of solid-state structure reported by Pickett and co-workers.[35] The Fe–Fe bond length of **1** (2.5710 Å) is close to that of its PDT analogue (2.555 Å), but significantly longer than those of its parent complex **A** (2.5159 Å) and its ODT analogue (2.5235 Å).[35,40]

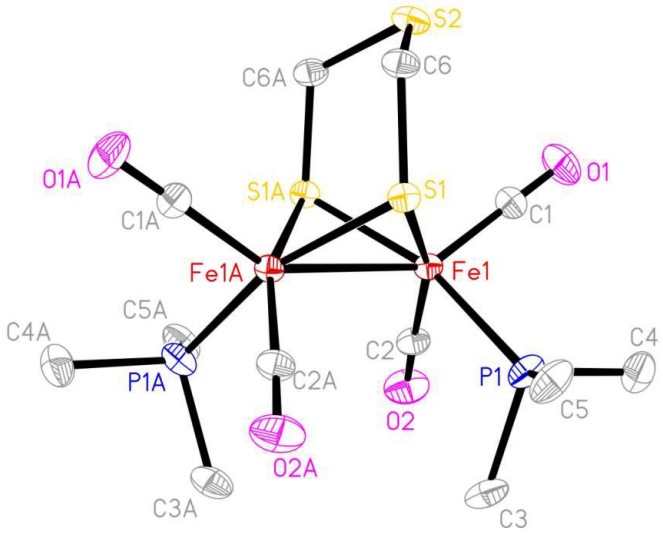

Fig. 2 Molecular structure of **1**. Hydrogen atoms are omitted for clarity. Ellipsoids are plotted at the 15% probability level.

Synthesis and characterization of μ-hydride-containing complexes $[(\mu\text{-TDT})Fe_2(CO)_4(PMe_3)_2(\mu\text{-H})]^+Y^-$ (2–7)

Although some diiron μ-hydride complexes have been prepared by protonation reactions of the PMe_3-disubstituted diiron complexes,[30-37] no protonation reaction of diiron complex $(\mu\text{-TDT})Fe_2(CO)_4(PMe_3)_2$ (**1**) and its product μ-hydride complex are

reported, up to now. Interestingly, we found that when complex **1** was treated with excess protic acids HY (Y = Cl, ClO_4, PF_6, BF_4, CF_3CO_2, CF_3SO_3) in MeCN at room temperature, the corresponding μ-hydride-containing cationic complex salts **2–7** were produced in 80–90% yields (Scheme 3).

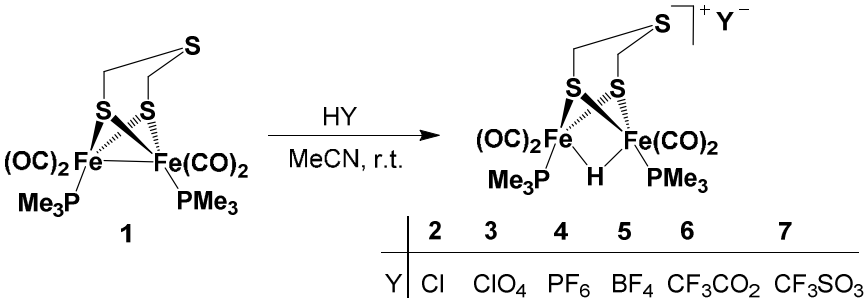

Scheme 3 Synthesis of complexes **2-7**

All the μ-hydride complexes **2–7** are air-stable red solids and have been characterized by elemental analysis and various spectroscopic techniques. The IR spectra of **2–7** each displayed only two strong absorption bands in the range 2041–1984 cm^{-1} for their terminal carbonyls. These bands are shifted towards much higher energy as compared to those of their precursor complex **1**, obviously owing to the decreased electron density at their Fe centers by protonation reactions with protic acids HY. The ^1H NMR spectra of **2–7** showed a doublet in the region 1.58–1.60 ppm for their CH_3 groups attached to P atoms and a triplet from −14.98 to −15.00 ppm for their bridging μ-H atoms.[34,35,42] The $^{31}P\{^1H\}$ NMR spectra of **2–7** exhibited a singlet in the region 21.04–21.14 ppm for P atoms in their PMe_3 ligands,[34,35,42] whereas **4** displayed an additional heptet at −144.61 ppm for the P atom in its $[PF_6]^-$ anion. In $^{19}F\{^1H\}$ NMR spectra, while **4** displayed a doublet at −72.93 ppm for F atoms in its $[PF_6]^-$ anion, **5** displayed two singlets at −151.78 and −151.73 with a 4:1 ratio

integrated intensity for its F atoms respectively bound to ^{11}B and ^{10}B atoms in its $[BF_4]^-$ anion.[43] In addition, **6** and **7** showed a singlet at −74.61 and −79.20 ppm for their F atoms in anions $[CF_3CO_2]^-$ and $[CF_3SO_3]^-$, respectively. It follows that, similar to their precursor complex **1**, all the spectroscopic data have proved that the isolated protonated products **2–7** each have only one type of isomer, namely the trans-ba/ba isomer, although they can exist as the ap/ba, cis-ba/ba, and trans-ba/ba isomers during the course of the protonation reactions (see below).

Fortunately, the molecular structures of **3–5** were confirmed unequivocally by X-ray crystallography. While their ORTEP plots are depicted in Figs. 3–5, Table S2 presents the selected bond lengths and angles. As can be seen in Figs. 3–5, the molecular structures of **3–5** are composed of one protonated complex cation $[(\mu\text{-TDT})Fe_2(CO)_4(PMe_3)_2(\mu\text{-H})]^+$ and the one corresponding anion. In the complex cation there is a μ-H atom bridged between its two iron centers, whereas its two PMe_3 ligands are located in basal positions of the two square-pyramidal metal centers with a trans coordination mode. In addition, both **3** and **5** contain a tetrahedral $[ClO_4]^-$ or $[BF_4]^-$ anion, whereas **4** has an octahedral anion $[PF_6]^-$. The metal-metal bond lengths of **3–5** are in the range 2.5721–2.5799 Å, which are very close to those of their precursor complex **1** (2.5710 Å) and their PDT analogue $[(\mu\text{-PDT})Fe_2(CO)_4(PMe_3)_2(\mu\text{-H})]^+[PF_6]^-$ (2.578 Å)[33], but obviously longer than the corresponding Fe–Fe bond length (2.55 Å) in the reduced state of [FeFe]Hases.[44]

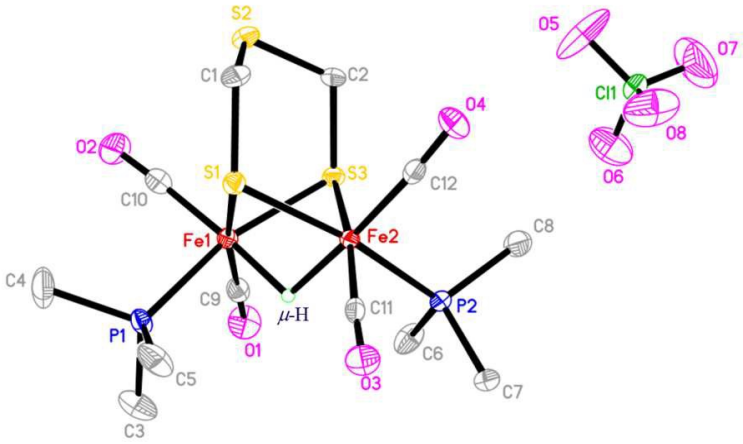

Fig. 3 Molecular structure of **3**. Except μ-H, the other hydrogen atoms are omitted for clarity. Ellipsoids are plotted at the 65% probability level.

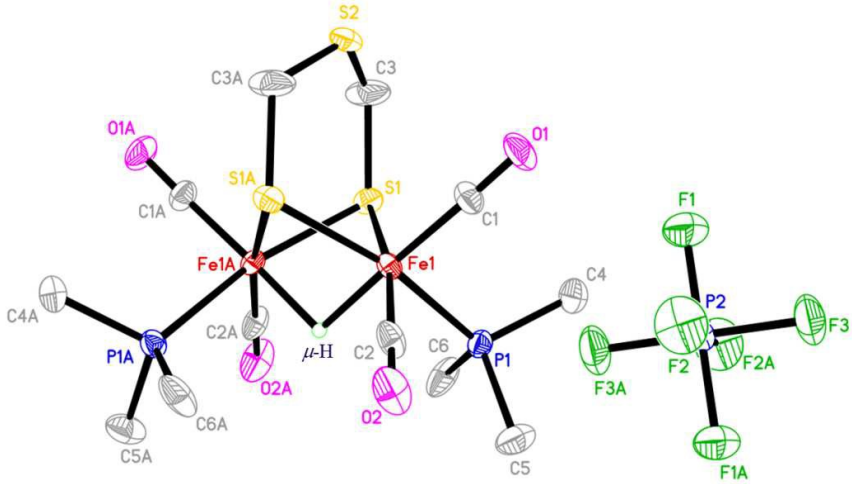

Fig. 4 Molecular structure of **4**. Except μ-H, the other hydrogen atoms are omitted for clarity. Ellipsoids are plotted at the 15% probability level.

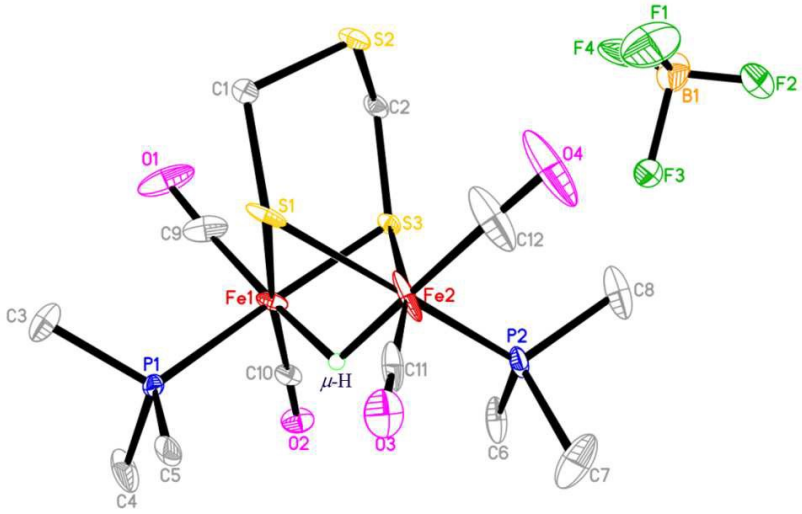

Fig. 5 Molecular structure of **5**. Except μ-H, the other hydrogen atoms are omitted for clarity. Ellipsoids are plotted at the 35% probability level.

Isomer type and stability of μ-hydride complexes 2-7 formed in situ by protonation reactions

As described above, through protonation reactions of complex **1** with the proton acids HY, a series of the cationic μ-hydride complexes **2–7** has been isolated and characterized as only the trans-ba/ba type isomers. Now, the questions are (i) whether or not the other three isomers (ap/ap, ap/ba, and cis-ba/ba) were formed during the course of the protonation reactions; (ii) if they were formed, how about their stability; and (iii) whether or not the less stable isomers could be converted to the more stable isomers. In order to answer these questions, we first determined the in situ ^{1}H and ^{31}P{^{1}H} NMR spectra of complexes **2–7** after the 5 min protonation reactions of complex **1** with HY acids in CD_3CN (see Fig. S1/Table S3 and Fig. S2/Table S4 for the NMR spectra and NMR data for their μ-H and trimethylphosphine's P atoms, respectively). As can be seen in Figs. S1/S2 and Tables S3/S4, (i) the 5 min

protonation reactions of complex **1** with HY acids did not give the ap/ap isomers of **2–7** since no μ-H and trimethylphosphine′s P signals appeared for this type of isomer (note that for the ap/ap isomer of their ODT analogue, the $\delta_{\mu\text{-H}} = -14.55$ ppm and $\delta_{PMe3} = 24.48$ ppm);[34,35,42] (ii) for **2** only the trans-ba/ba isomer was formed; (iii) for **6** the trans-ba/ba and ap/ba isomers were formed with a molar ratio trans-ba/ba > ap/ba (see Tables S3/S4 for the specific values); and (iv) for **3–5** and **7** the trans-ba/ba, ap/ba, and cis-ba/ba isomers were formed with a molar ratio of trans-ba/ba > ap/ba > cis-ba/ba (see Tables S3/S4 for the specific values,). It follows that among the four possible isomers of **2–7**, the ap/ap isomer is the most unstable one and even could not be detected by in situ ^{1}H and ^{31}P $\{^{1}$H$\}$ NMR spectroscopy (note that the highest instability of ap/ap isomer is due to the strong steric repulsions between its TDT ligand and the two apical PMe_3 ligands).[40] In addition, according to the molar ratio of the other three isomers, the trans-ba/ba isomer is most stable since it does not have the steric repulsion between its TDT ligand and the two basal PMe_3 ligands located with a trans arrangement.

To answer the third question mentioned above, we further determined the in situ ^{1}H and ^{31}P$\{^{1}$H$\}$ NMR spectra of complex **5** at different time of the protonation reaction of **1** with $HBF_4{\cdot}Et_2O$ from 5 min to 85 min (see Fig. S3/Table S5 and Fig. 4/Table S6 for the NMR spectra and NMR data of μ-H and trimethylphosphine's P atoms of **5**, respectively). As can be seen in Figs. S3/S4 and Tables S5/S6, (i) the reaction mixtures generated by protonation reactions of **1** with $HBF_4{\cdot}Et_2O$ from 5 to 45 min all contained the ap/ba, cis-ba/ba, and trans-ba/ba isomers of **5**; (ii) while the

ap/ba and cis-ba/ba isomers of **5** were gradually decreased from 5 to 45 min, the trans-ba/ba isomer of **5** was gradually increased from 5 to 45 min; and (iii) after the 85 min protonation reaction, the former two less stable isomers were disappeared and completely converted to the most stable trans-ba/ba isomer with a triplet at −14.99 ppm for its μ-H and a singlet at 21.10 ppm for its trimethylphosphine's P atoms. Apparently, such observations are in good agreement with the fact that only the trans-ba/ba isomers of **2–7** were isolated from the reaction mixtures formed by protonation reactions of complex **1** with the corresponding HY acids.

Finally, it should be noted that anions Y^- in **3–7** play an important role for stabilization of the less stable isomers, but anion Cl^- in **2** does not have such a kind of stabilization effect. Thus, (i) when Y^- = Cl^- in **2**, only the most stable isomer trans-ba/ba was observed; (ii) when Y^- = $CF_3CO_2^-$ in **6**, the less stable isomer ap/ba was also observed; and (iii) when Y^- = ClO_4^-, PF_6^-, BF_4^-, and $CF_3SO_3^-$ in **3–5** and **7**, the less stable ap/ba and cis-ba/ba isomers were all observed (see Figs S1/S2 and Tables S3 and S4). This implies that the stabilization intensity of anions Y^- is in the order: the four anions in **3–5** and **7** > anion $CF_3CO_2^-$ in **6** > anion Cl^- in **2**. However, according to the protonated isomer ratios we cannot arrange an exact stabilization intensity order for the four anions in **3–5** and **7**, since the isomer ratios are not derectly related to their stabilization intensity.

H/D exchange reactions between μ-hydride complex 7 and deuterium reagents

Up to now, the H/D exchange reactions of the [Fe^{II}(μ-H)Fe^{II}]-type μ-hydride

complexes with some deuterium reagents such as D_2 and D_2O have been used to test whether or not such complexes can act as the functional models of [FeFe]Hases for H_2-binding and activation.[33,40,41] Therefore in order to test whether or not our model complexes **2–7** of this type have the H_2 activation ability, we chose **7** as a representative complex (due to its higher photostability and better solubility in common organic solvents) to study the H/D exchange reactions with deuterium reagents D_2, D_2O, and DCl according to eqs 1–3, where **8** represents $[(\mu\text{-TDT})Fe_2(CO)_4(PMe_3)_2(\mu\text{-D})]^+[CF_3SO_3]^-$.[40,41,45-47]

$$\mathbf{7} + D_2 \rightarrow \mathbf{8} + HD \qquad (1)$$

$$\mathbf{7} + D_2O \rightarrow \mathbf{8} + HOD \qquad (2)$$

$$\mathbf{7} + DCl \rightarrow \mathbf{8} + HCl \qquad (3)$$

As a result, we found that the H/D exchange between **7** and D_2 or D_2O cannot occur (see SI for discussion of the unsuccessful H/D exchange results), while the H/D exchange of **7** with DCl has been proved to take place immediately and almost quantitatively (see below) to give the expected H/D exchange product **8**. This implies that the H/D exchange of **7** with DCl does not require an activation step of DCl by complex **7** (in contrast to this, the H/D exchange reactions of some protonated diiron complexes with D_2 are known via an activation step of D_2).[40,41] This H/D exchange experiment was carried out in an NMR tube containing an acetone or acetone-d_6 solution of **7** and an equimolar DCl in the dark for 5 min or under irradiation of ambient laboratory light for 5 min. The in situ ^2H and $^{31}P\{^1H\}$ NMR spectra of the resulting mixture showed the μ-D signal ($\delta_{\mu\text{-D}}$: a triplet at −14.33 ppm with $J_{D\text{-}P}$ = 3.23 Hz) and $^{31}P\{^1H\}$ NMR signal (δ_P: a triplet at 21.61 ppm with $J_{P\text{-}D}$ = 3.23 Hz for P in

PMe_3) (see Figs. 6 and 7). In addition, Fig. 6 also shows the ^2H NMR signals for solvent D_2O (δ_D: a singlet at 2.63 ppm), unreacted DCl (δ_D: a singlet at 4.83 ppm), and some HOD (δ_D: a singlet at 1.99 ppm) formed presumably by reaction of the in situ generated HCl with solvent D_2O.

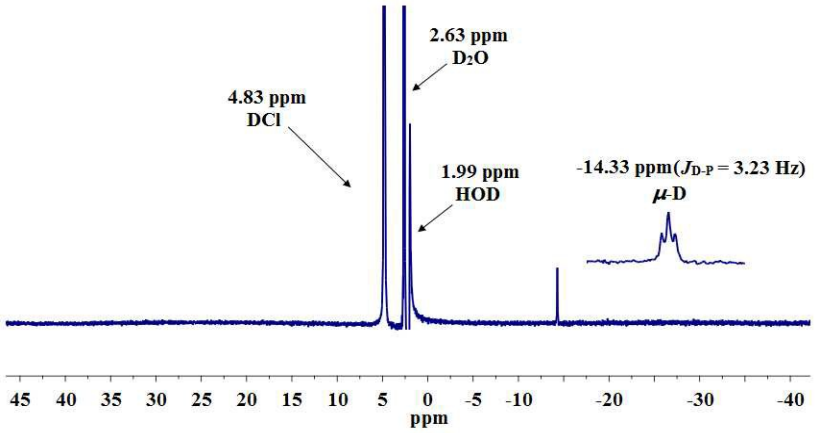

Fig. 6 In situ ^2H NMR spectrum of **8** taken after the 5 min H/D exchange reaction of **7** with DCl.

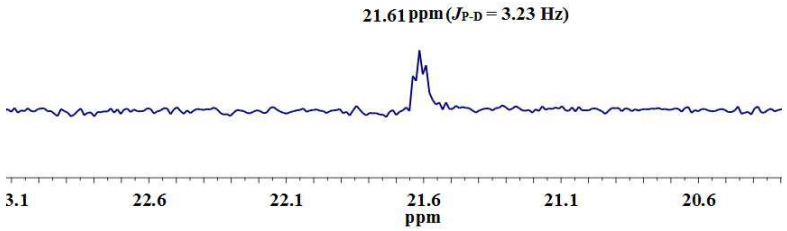

Fig. 7 In situ $^{31}P\{^1H\}$ NMR spectrum of **8** taken after the 5 min H/D exchange reaction of **7** with DCl.

Isolation and characterization of μ-deuterium-containing complex 8

To further confirm the structure of complex **8**, we have isolated **8** from the H/D exchange reaction of complex **7** with 1 equiv of DCl in an acetone-d_6 followed by treatment with CF_3SO_3Ag (note that adding CF_3SO_3Ag is to obtain the pure **8**

containing only the $CF_3SO_3^-$ anion by removing anion Cl^- derived from DCl as a precipitate AgCl) at room temperature in 90% yield. Complex **8** is an air-stable red solid and has been fully characterized by elemental analysis, spectroscopy, and X-ray diffraction analysis. The IR spectrum of **8** showed two strong absorption bands at 1991 and 2032 cm^{-1} for its terminal carbonyls, which is very similar to those of its precursor **7** and the previously reported μ-hydride analogues.[33,40] The ^1H NMR spectrum of **8** displayed a doublet at 1.72 ppm with $J_{P\text{-}H}$ = 10.4 Hz for Me groups in its PMe_3 ligands. Similar to the in situ ^2H NMR determination indicated above, the ^2H NMR spectrum of isolated **8** showed a triplet at −14.52 ppm in the high field resulting from the coupling between its P atom and μ-D ($J_{P\text{-}D}$ = 3.23 Hz). In addition, the ^{31}P $\{^1H\}$ NMR spectrum of isolated **8** also exhibited a triplet at 21.59 ppm resulting from the coupling between its P atom and μ-D with the same coupling constant ($J_{D\text{-}P}$ = 3.23 Hz).

The molecular structure of **8** determined by X-ray crystallography is shown in Fig. 8. Table S7 lists its selected bond lengths and angles. As can be seen in Figure 8, the μ-deuterium complex **8** is structurally very similar to its μ-hydride analogues **3–5** and the previously reported μ-hydride analogues.[33] Complex **8** indeed contains one $[CF_3SO_3]^-$ anion and one $[(\mu\text{-TDT})Fe_2(CO)_4(PMe_3)_2(\mu\text{-D})]^+$ complex cation in which there is a deuterium atom bridged between the two square-pyramidal Fe centers and there are two PMe_3 ligands lying in the basal positions of the two Fe centers with a trans coordination mode. In addition, the Fe–Fe bond length of complex **8** (2.5866 Å) is very close to those of its μ-hydride analogues **3–5** (2.5721–2.5799 Å), but

obviously shorter than those of the oxidized state of [FeFe]Hases (2.60–2.62 Å).[5,6] To our knowledge, complex **8** is the first crystallographically characterized μ-deuterium-containing butterfly [2Fe2S] cluster complex, although a few of such a type of complexes were previously characterized spectroscopically.[33,40,48]

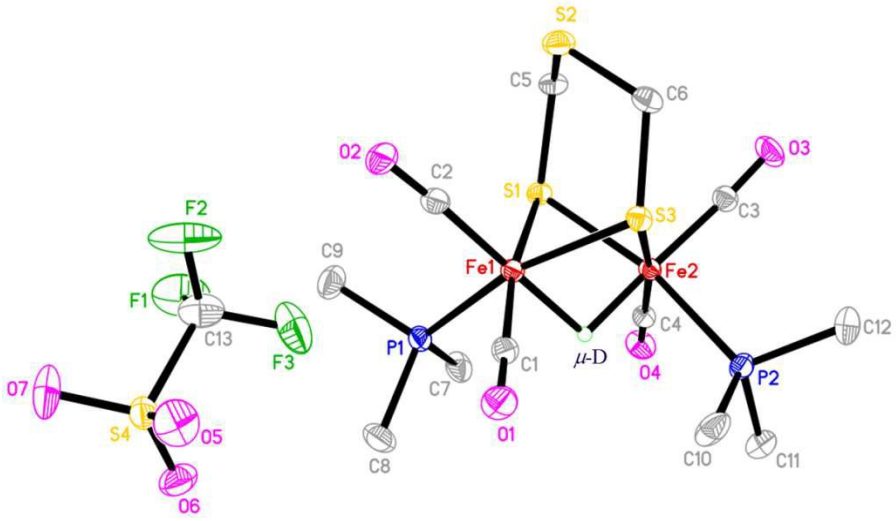

Fig. 8 Molecular structure of **8**. Hydrogen atoms are omitted for clarity. Ellipsoids are plotted at the 15% probability level.

Summary and conclusion

We have synthesized the first thiodithiolate (TDT) ligand-containing μ-hydride complexes **2–7** by protonation reactions of the PMe_3-disubstituted complex **1** with the corresponding acids. The prepared μ-hydride complexes **2–7** might be able to serve as good models for the protonated diiron subsite of [FeFe]Hases. This is because (i) the central S atom-containing dithiolate TDT-bridged butterfly [2Fe2S] cluster in **2–7** is very similar to the heteroatom N-containing ADT-bridged diiron subsite in [FeFe]Hases; (ii) the two electron-donating PMe_3 ligands with a trans-ba/ba arrangement in **2–7** much resemble the two CN^- ligands located with a trans

coordination mode in the diiron subsite of the natural enzymes; and (iii) the protonated diiron subsite of [FeFe]Hases is reported to be an intermediate during the catalytic H_2 production. Particularly interesting is that while the isolated μ-hydride complexes **2–7** have been proved to contain only the trans-ba/ba isomers, the in situ ^1H and $^{31}P\{^1H\}$ NMR measurements of the mixtures produced by the 5 min protonation reactions of complex **1** with the corresponding acids reveal that (i) products **2–7** do not have the ap/ap isomers; (ii) product **2** contains only the trans-ba/ba isomer; (iii) product **6** contains two isomers with a molar ratio of trans-ba/ba > ap/ba; (iv) products **3–5** and **7** contain three isomers with a molar ratio trans-ba/ba > ap/ba > cis-ba/ba. In addition, the in situ ^1H and $^{31}P\{^1H\}$ NMR determinations of the mixtures generated by the 5–85 min protonation reactions of complex **1** with $HBF_4{\cdot}Et_2O$ indicate that the less stable ap/ba and cis-ba/ba isomers can be converted to the most stable trans-ba/ba isomer. Apparently, such observations can provide not only an explanation why only the trans-ba/ba isomers of **2–7** can be isolated from the protonation reaction mixtures, but also provide a better understanding of the formation of the protonated intermediates and their possible isomerization during the course of H_2 production catalyzed by [FeFe]Hases. It should be noted that although the H/D exchange of **7** with D_2 or D_2O has been proved not to occur under the studied conditions, the H/D exchange between **7** and DCl proceeds immediately to give the expected μ-deuterium complex $[(\mu\text{-TDT})Fe_2(CO)_4(PMe_3)_2(\mu\text{-D})]^+[CF_3SO_3]^-$ (**8**) in an almost quantitative yield. All the new complexes **1–8** have been fully characterized by elemental analysis and

various spectroscopic methods, and particularly for some of them by X-ray diffraction analysis.

Experimental section

General comments

All manipulations were performed using standard Schlenk and vacuum-line techniques under N_2 or in a N_2-filled glovebox. MeCN was distilled under N_2 once from P_2O_5 and then from CaH_2, whereas Et_2O and hexane were distilled under N_2 from sodium/benzophenone ketyl. While (μ-TDT)$Fe_2(CO)_6$ (**A**) was prepared according to the published procedure,[38] PMe_3 (1 M in THF), 37% HCl, 70% $HClO_4$, 60% HPF_6, 50% $HBF_4{\cdot}Et_2O$, CF_3CO_2H, CF_3SO_3H, DCl (20% wt in D_2O) and the other materials were commercially available and used as received. IR spectra were recorded on a Bruker Tensor 27 FT-IR infrared spectrophotometer. ^1H, $^{31}P\{^1H\}$, $^{19}F\{^1H\}$, $^{11}B\{^1H\}$ NMR spectra were taken on a Bruker Avance 400 NMR spectrometer. ^2H NMR spectra were taken on a Bruker Avance 600 NMR spectrometer operating at 92.2 MHz. Elemental analyses were performed with an Elementar Vario EL analyzer. Melting points were determined on a SGW X-4 microscopic melting point apparatus and were uncorrected.

Preparation of (μ-TDT)$Fe_2(CO)_4(PMe_3)_2$ (1)

A 50 mL, three-necked flask equipped with a stir-bar, a serum cap, and a reflux condenser topped with an N_2 inlet tube was charged with (μ-TDT)$Fe_2(CO)_6$ (**A**) (0.202 g, 0.5 mmol), PMe_3 (2.5 mL, 2.5 mmol), and hexane (15 mL). The stirred

mixture was refluxed for 2 h and then cooled to room temperature. The resulting dark-red solution was subjected to column chromatography (silica gel) under anaerobic conditions. Elution with CH_2Cl_2/hexane (1:2, v/v) developed a major red band, from which **1** (0.200 g, 80%) was obtained as a red solid, mp 114–115 °C. Anal. Calcd for $C_{12}H_{22}Fe_2O_4P_2S_3$: C, 28.82; H, 4.43. Found: C, 28.90; H, 4.38. IR (KBr disk): $\nu_{C\equiv O}$ 1979 (m), 1944 (vs), 1898 (vs) cm^{-1}. ^1H NMR (400 MHz, CD_3CN): 1.56 (d, $^2J_{P\text{-}H}$ = 9.2 Hz, 18H, $2(CH_3)_3$), 3.22 (s, 4H, $2SCH_2S$) ppm. $^{31}P\{^1H\}$ NMR (162 MHz, CD_3CN, 85% H_3PO_4): 22.2 (s, $2PMe_3$) ppm.

Preparation of $[(\mu\text{-TDT})Fe_2(CO)_4(PMe_3)_2(\mu\text{-H})]^+Cl^-$ (2)

A 50 mL, three-necked flask fitted with a stir-bar, two serum caps, and an N_2 inlet tube was charged with **1** (0.250 g, 0.5 mmol) and MeCN (20 mL). To the resulting dark-red solution was added 37% concentrated HCl (0.42 mL, 5.0 mmol) by syringe, causing an immediate color change from dark-red to orange-red. After the orange-red solution was stirred at room temperature for additional 15 min, it was evaporated to dryness under vacuum. The residue was washed with ether (10 mL×5) and finally dried under vacuum to give **2** (0.220 g, 82%) as a red solid, mp 75 °C (dec). Anal. Calcd for $C_{12}H_{23}ClFe_2O_4P_2S_3$: C, 26.86; H, 4.32. Found: C, 26.83; H, 4.42. IR (KBr disk): $\nu_{C\equiv O}$ 2041 (vs), 1988 (vs) cm^{-1}. ^1H NMR (400 MHz, CD_3CN): −15.00 (t, $^2J_{P\text{-}H}$ = 21.6 Hz, 1H, Fe–H–Fe), 1.60 (d, $^2J_{P\text{-}H}$ =10.8 Hz, 18H, $2P(CH_3)_3$), 3.67–3.76 (m, 4H, $2SCH_2S$) ppm. $^{31}P\{^1H\}$ NMR (162 MHz, CD_3CN, 85% H_3PO_4): 21.1 (s, $2PMe_3$) ppm.

Preparation of $[(\mu\text{-TDT})Fe_2(CO)_4(PMe_3)_2(\mu\text{-H})]^+[ClO_4]^-$ (3)

The same equipped flask as for **2** was charged with **1** (0.250 g, 0.5 mmol) and MeCN (20 mL). To the resulting dark-red solution was added $HClO_4$ (0.41 mL, 5.0 mmol) by syringe, causing an immediate color change from dark-red to orange-red. The orange-red solution was stirred at room temperature for additional 1.5 h. After the same workup as for **2**, complex **3** (0.270 g, 90%) was obtained as a red solid, mp 146 °C (dec). Anal. Calcd for $C_{12}H_{23}ClFe_2O_8P_2S_3$: C, 24.00; H, 3.86. Found: C, 23.89; H, 3.96. IR (KBr disk): $\nu_{C\equiv O}$ 2028 (s), 1984 (s) cm^{-1}. ^1H NMR (400 MHz, CD_3CN): −14.99 (t, $^2J_{P\text{-}H}$ = 21.2 Hz, 1H, Fe–H–Fe), 1.60 (d, $^2J_{P\text{-}H}$ = 10.0 Hz, 18H, $2P(CH_3)_3$), 3.68–3.76 (m, 4H, $2SCH_2S$) ppm. $^{31}P\{^1H\}$ NMR (162 MHz, CD_3CN, 85% H_3PO_4): 21.1 (s, $2PMe_3$) ppm.

Preparation of $[(\mu\text{-TDT})Fe_2(CO)_4(PMe_3)_2(\mu\text{-H})]^+[PF_6]^-$ (4)

The same equipped flask as for **2** was charged with **1** (0.250 g, 0.5 mmol) and MeCN (20 mL). To the resulting dark-red solution was added 60% HPF_6 (0.70 mL, 5.0 mmol) to cause an immediate color change from dark-red to orange-red. The orange-red solution was stirred at room temperature for additional 1.5 h. The same workup as for **2** afforded complex **4** (0.290 g，90%) as a red solid, mp 195 °C (dec). Anal. Calcd for $C_{12}H_{23}F_6Fe_2O_4P_3S_3$: C, 22.31; H, 3.59. Found: C, 22.33; H, 3.44. IR (KBr disk): $\nu_{C\equiv O}$ 2035 (vs), 1991 (vs) cm^{-1}. ^1H NMR (400 MHz, CD_3CN): −15.00 (t, $^2J_{P\text{-}H}$ = 21.6 Hz, 1H, Fe–H–Fe), 1.60 (d, $^2J_{P\text{-}H}$ = 10.4 Hz, 18H, $2(CH_3)_3$), 3.67–3.76 (m, 4H, $2SCH_2S$) ppm. $^{31}P\{^1H\}$ NMR (162 MHz, CD_3CN, 85% H_3PO_4): 21.0 (s, $2PMe_3$), −144.6 (heptet, $J_{F\text{-}P}$ = 706 Hz, PF_6) ppm. $^{19}F\{^1H\}$ NMR (376 MHz, CD_3CN, $CFCl_3$): −72.9 (d, $J_{P\text{-}F}$ = 706 Hz, PF_6) ppm.

Preparation of [(μ-TDT)$Fe_2(CO)_4(PMe_3)_2$(μ-H)]$^+$[BF_4]$^-$ (5)

The same equipped flask as for **2** was charged with **1** (0.250 g, 0.5 mmol) and MeCN (20 mL). To the resulting dark-red solution was added $HBF_4 \cdot Et_2O$ (0.60 mL, 5.0 mmol) by a syringe, causing an immediate color change from dark-red to orange-red. The orange-red solution was stirred at room temperature for additional 1.5 h. After the same workup as for **2**, complex **5** (0.255 g, 87%) was obtained as a red solid, mp173 °C (dec). Anal. Calcd for $C_{12}H_{23}BF_4Fe_2O_4P_2S_3$: C, 24.51; H, 3.94. Found: C, 24.63; H, 4.06. IR (KBr disk): $\nu_{C\equiv O}$ 2031 (vs), 1990 (vs) cm^{-1}. ^1H NMR (400 MHz, CD_3CN): −14.98 (t, $^2J_{P\text{-}H}$ = 21.6 Hz, 1H, Fe–H–Fe), 1.60 (d, $^2J_{P\text{-}H}$ = 10.0 Hz, 18H, $2(CH_3)_3$), 3.67−3.75 (m, 4H, $2SCH_2S$) ppm. $^{31}P\{^1H\}$ NMR (162 MHz, CD_3CN, 85% H_3PO_4): 21.1 (s, $2PMe_3$) ppm. $^{11}B\{^1H\}$ NMR (128 MHz, CD_3CN, $BF_3 \cdot Et_2O$): −1.19 (s) ppm. $^{19}F\{^1H\}$ NMR (376 MHz, CD_3CN, $CFCl_3$): −151.78 (s, $^{11}BF_4$), −151.73 (s, $^{10}BF_4$) ppm.

Preparation of [(μ-TDT)$Fe_2(CO)_4(PMe_3)_2$(μ-H)]$^+$[CF_3CO_2]$^-$ (6)

The same equipped flask as for **2** was charged with **1** (0.250 g, 0.5 mmol), MeCN (20 mL) and MeOH (10 mL) to produce a dark-red solution. To the stirred dark-red solution was added CF_3CO_2H (3.70 mL, 50.0 mmol) via a syringe, resulting in a gradual color change from dark-red to orange-red. After the orange-red solution was stirred at room temperature for additional 2 h, it was evaporated to dryness under vacuum. The residue was washed with ether (5 mL×5) and finally dried under vacuum to give **6** (0.245 g, 80%) as a red solid, mp 69 °C (dec). Anal. Calcd for $C_{14}H_{23}F_3Fe_2O_6P_2S_3$: C, 27.38; H, 3.77. Found: C, 27.52; H, 3.61. IR (KBr disk): $\nu_{C\equiv O}$

2025 (vs), 1986 (vs) cm^{-1}. ^{1}H NMR (400 MHz, CD_3CN): −14.98 (t, $^{2}J_{P\text{-}H}$ = 21.6 Hz, 1H, Fe–H–Fe), 1.58 (d, $^{2}J_{P\text{-}H}$ =10.8 Hz, 18H, $2P(CH_3)_3$), 3.66–3.75 (m, 4H, $2SCH_2S$) ppm. $^{31}P\{^{1}H\}$ NMR (162 MHz, CD_3CN, 85% H_3PO_4): 21.1 (s, $2PMe_3$) ppm. $^{19}F\{^{1}H\}$ NMR (376 MHz, CD_3CN, $CFCl_3$): −74.6 (s, CF_3CO_2) ppm.

Preparation of $[(\mu\text{-TDT})Fe_2(CO)_4(PMe_3)_2(\mu\text{-H})]^{+}[CF_3SO_3]^{-}$ (7)

The same equipped flask as for **2** was charged with **1** (0.250 g, 0.5 mmol) and MeCN (20 mL). To the stirred dark-red solution was added CF_3SO_3H (0.44 mL, 5.0 mmol) by syringe, causing an immediate color change from dark-red to orange red. The orange-red solution was stirred at room temperature for additional 1.5 h. The same workup as for **2** produced complex **7** (0.293 g, 90%) as a red solid, mp 162 °C (dec). Anal. Calcd for $C_{13}H_{23}F_3Fe_2O_7P_2S_4$: C, 24.01; H, 3.57. Found: C, 24.22; H, 3.79. IR (KBr disk): $\nu_{C\equiv O}$ 2035 (vs), 1990 (vs) cm^{-1}. ^{1}H NMR (400 MHz, CD_3CN): −14.99 (t, $^{2}J_{P,H}$ = 21.4 Hz, 1H, Fe–H–Fe), 1.60 (d, $^{2}J_{P\text{-}H}$ = 9.6 Hz, 18H, $2P(CH_3)_3$), 3.68–3.76 (m, 4H, $2SCH_2S$) ppm. $^{31}P\{^{1}H\}$ NMR (162 MHz, CD_3CN, 85% H_3PO_4): 21.1 (s, $2PMe_3$) ppm. $^{19}F\{^{1}H\}$ NMR (376 MHz, CD_3CN, $CFCl_3$): −79.2 (s, CF_3SO_3) ppm.

In situ monitor of isomer type and stability of μ-hydride complexes 2–7 in CD_3CN

To a CD_3CN (0.5 mL) solution of complex **1** (5.0 mg, 0.01 mmol) in an NMR tube was added a CD_3CN (0.2 mL) solution of 10 equiv of 37% HCl, 70% $HClO_4$, 60% HPF_6, 50% $HBF_4{\cdot}Et_2O$, or CF_3SO_3H, or a CD_3CN (0.2 mL) solution of 100 equiv of CF_3CO_2H (due to its weak acidity). After the 5 min protonation reactions, the ^{1}H and $^{31}P\{^{1}H\}$ NMR spectra of the prepared samples were immediately recorded (see Figs.

S1/S2 and Tables S3/S4). Similarly, the ^{1}H and $^{31}P\{^{1}H\}$ NMR spectra of the sample prepared by protonation reaction of complex **1** with 10 equiv of 50% $HBF_4{\cdot}Et_2O$ in CD_3CN were determinated during the course of 5−85 min (see Figs. S3/S4 and Tables S5/S6).

In situ monitor of H/D exchange reaction between 7 and D_2

A CD_2Cl_2 (0.5 mL) or CH_2Cl_2 (0.5 mL) solution of **7** (40 mg, 0.06 mmol) was added to a J-Young NMR tube. The tube was frozen, evacuated, and back-filled with 2 bar D_2. After the frozen sample was warmed to room temperature, the sample solution was left in the dark or irradiated with ambient laboratory light. The ^{1}H and ^{2}H NMR spectra of the prepared samples were taken at the specified time and proved that the H/D exchange reaction between **7** and D_2 did not occur under such conditions (see SI for discussion of this unsuccessful H/D exchange results).

In situ monitor of H/D exchange reaction between 7 and D_2O

To an acetone-d_6 (0.5 mL) or acetone (0.5 mL) solution of **7** (40 mg, 0.06 mmol) in an NMR tube was added D_2O (20 μL, 1.10 mmol). The sample solution was left in the dark or irradiated by exposure to ambient laboratory light. The ^{1}H and ^{2}H NMR spectra of the prepared samples were determined at the specified time, which proved that the H/D exchange reaction between **7** and D_2O did not take place under such conditions (see SI for discussion of this unsuccessful H/D exchange results).

In situ monitor of H/D exchange reaction between 7 and DCl

To an acetone-d_6 (0.5 mL)or acetone (0.5 mL) solution of **7** (40 mg, 0.06 mmol) in an

NMR tube was added DCl (10 μL) solution (20% wt in D_2O, 0.06 mmol) and then the tube was kept in the dark or exposed to ambient laboratory light for 5 min. The ^1H, ^2H, and $^{31}P\{^1H\}$ NMR spectra of the prepared samples proved the formation of the expected H/D exchange product $[(\mu\text{-TDT})Fe_2(CO)_4(PMe_3)_2(\mu\text{-D})]^+[CF_3SO_3]^-$ (**8**) during the course of the H/D exchange reactions under such conditions.

Isolation and characterization of $[(\mu\text{-TDT})Fe_2(CO)_4(PMe_3)_2(\mu\text{-D})]^+[CF_3SO_3]^-$ (8)

A 25 mL, Schlenk flask was charged with an acetone-d_6 (1 mL) solution of **7** (0.080 g, 0.12 mmol) and 20 μL of DCl solution (20% wt DCl in D_2O, 0.12 mmol). After the mixed solution was stirred at room temperature for 15 min, CF_3SO_3Ag (0.031 g, 0.12 mmol) was added to give a white precipitate, immediately. The mixture was stirred at room temperature for additional 15 min and then it was centrifuged to remove the white precipitate AgCl. The collected orange-red solution was evaporated to dryness under vacuum. The residue was washed with 10 mL of ether and 2 × 20 mL of CH_2Cl_2/hexane (1:3, v/v) and finally dried under vacuum to give **8** (0.072 g, 90%) as a red solid, mp 146 °C (dec). Anal. Calcd for $C_{13}H_{22}DF_3Fe_2O_7P_2S_4$: C, 23.98; H, 3.71. Found: C, 23.74; H, 3.59. IR (KBr disk): $\nu_{C\equiv O}$ 2032 (vs), 1991 (vs) cm^{-1}. ^1H NMR (400 MHz, CD_3COCD_3): 1.72 (d, $^2J_{P\text{-}H}$ = 10.4 Hz, 18H, $2P(CH_3)_3$), 3.83–3.92 (m, 4H, $2SCH_2S$) ppm. $^{31}P\{^1H\}$ NMR (162 MHz, CD_3COCD_3, 85% H_3PO_4): 21.6 (t, $^2J_{P\text{-}D}$ = 3.23 Hz, $2PMe_3$) ppm. $^{19}F\{^1H\}$ NMR (376 MHz, CD_3COCD_3, $CFCl_3$): −78.0 (s, CF_3SO_3) ppm. ^2H NMR (92.2 MHz, CH_3COCH_3): −14.52 (t, $^2J_{P\text{-}D}$ = 3.23 Hz) ppm.

X-ray structure determinations of 1, 3–5, and 8

Single crystals suitable for X-ray diffraction analyses were grown by slow

evaporation of a hexane solution of **1** at −20 °C, slow diffusion of hexane into a CH_2Cl_2 solution of **3**, **5** or **8** at room temperature, and slow diffusion of ether into an acetone solution of **4** in the dark at room temperature. All the single crystals were mounted on a Bruker APEX II or a Bruker P4 diffractometer. Data were collected at room temperature using a confocal monochromator with Mo-Kα radiation (λ = 0.71073 Å) in the ω-2θ scanning mode. Data collection, reduction, and absorption correction were performed by CRYSTALCLEAR program.[49] The structures were solved by direct methods using the SHELXS-97 program[50] and refined by full-matrix least-squares techniques (SHELXL-97)[51] on F^2. Hydrogen and deuterium atoms were located by using the geometric method. Details of crystal data, data collections and structure refinements are summarized in Tables S8 and S9.

Acknowledgements

We are grateful to the Ministry of Science and Technology of China (973 programs 2014CB845604 and 2011CB935902) and the National Natural Science Foundation of China (21132001 and 21272122) for financial support of this work.

References

1 M. W. W. Adams and E. I. Stiefel, *Science*, 1998, **282**, 1842-1843.

2 R. Cammack, *Nature*, 1999, **397**, 214-215.

3 M. Frey, *ChemBioChem*, 2002, **3**, 153-160.

4 J. Alper, *Science*, 2003, **299**, 1686-1687.

5 J. W. Peters, W. N. Lanzilotta, B. J. Lemon and L. C. Seefeldt, *Science*, 1998, **282**, 1853-1858.

6 Y. Nicolet, C. Piras, P. Legrand, C. E. Hatchikian and J. C. Fontecilla-Camps, *Structure*, 1999, **7**, 13-23.

7 A. S. Pandey, T. V. Harris, L. J. Giles, J. W. Petters and R. K. Szilagyi, *J. Am. Chem. Soc.*, 2008, **130**, 4533-4540.

8 A. Silakov, B. Wenk, E. Reijerse and W. Lubitz, *Phys. Chem. Chem. Phys*., 2009, **11**, 6592-6599.

9 G. Berggren, A. Adamska, C. Lambertz, T. R. Simmons, J. Esselborn, M. Atta, S. Gambarelli, J.-M. Mouesca, E. Reijerse, W. Lubitz, T. Happe, V. Artero and M. Fontecave, *Nature*, 2013, **499**, 66-69.

10 For reviews, see for example: (a) W. Lubitz, H. Ogata, O. Rüdiger and E. Reijerse, *Chem. Rev*., 2014, **114**, 4081-4148; (b) T. R. Simmons, G. Berggren, M. Bacchi, M. Fontecave and V. Artero, *Coord. Chem. Rev*., 2014, **270-271**, 127-150; (c) C. Tard and C. J. Pickett, *Chem. Rev.*, 2009, **109**, 2245-2274; (d) J. C. Fontecilla-Camps, A. Volbeda, C. Cavazza and Y. Nicolet, *Chem. Rev.*, 2007, **107**, 4273-4303; (e) J.-F. Capon, F. Gloaguen, P. Schollhammer and J. Talarmin, *Coord. Chem. Rev.*, 2005, **249**, 1664-1676; (f) L.-C. Song, *Acc. Chem. Res*., 2005, **38**, 21-28; (g) M. Y. Darensbourg, E. J. Lyon, X. Zhao and I. P. Georgakaki, *PNAS*, 2003, **100**, 3683-3688.

11 F. Gloaguen, J. D. Lawrence, M. Schmidt, S. R. Wilson and T. B. Rauchfuss, *J. Am. Chem. Soc*., 2001, **123**, 12518-12527.

12 E. J. Lyon, I. P. Georgakaki, J. H. Reibenspies and M. Y. Darensbourg, *J. Am. Chem. Soc.*, 2001, **123**, 3268-3278.

13 M. Razavet, S. C. Davies, D. L. Hughes, J. E. Barclay, D. J. Evans, S. A. Fairhurst, X. Liu and C. J. Pickett, *Dalton Trans*., 2003, 586-595.

14 C. Tard, X. Liu, S. K. Ibrahim, M. Bruschi, L. De Giola, S. C. Davies, X. Yang, L.-S. Wang, G. Sawers and C. J. Pickett, *Nature*, 2005, **433**, 610-613.

15 C. M. Thomas, T. Liu, M. B. Hall and M. Y. Darensbourg, *Inorg. Chem.*, 2008, **47**, 7009-7024.

16 J. D. Lawrence, H. Li, T. B. Rauchfuss, M. Bénard and M.-M. Rohmer, *Angew. Chem. Int. Ed*., 2001, **40**, 1768-1771.

17 H. Li and T. B. Rauchfuss, *J. Am. Chem. Soc*., 2002, **124**, 726-727.

18 W. Dong, M. Wang, T. Liu, X. Liu, K. Jin and L. Sun, *J. Inorg. Biochem*., 2007, **101**, 506-513.

19 J.-F. Capon, S. Ezzaher, F. Gloaguen, F. Y. Pétillon, P. Schollhammer and J. Talarmin, *Chem. Eur. J*., 2008, **14**, 1954-1964.

20 J. Windhager, M. Rudolph, S. Bräutigam, H. Görls and W. Weigand, *Eur. J. Inorg. Chem*., 2007, 2748-2760.

21 U.-P. Apfel, Y. Halpin, M. Gottschaldt, H. Görls, J. G. Vos and W. Weigand, *Eur. J. Inorg. Chem.*, 2008, 5112-5118.

22 M. K. Harb, T. Niksch, J. Windhager, H. Görls, R. Holze, L. T. Lochett, N. Okumura, D. H. Evans, R. S. Glass, D. L. Lichtenberger, M. El-khateeb and W. Weigand, *Orgamometallics*, 2009, **28**, 1039-1048.

23 J. M. Camara and T. B. Rauchfuss, *Nat. Chem.*, 2012, **4**, 26-30.

24 L. R. Almazahreh, U-P. Apfel, W. Imhof, M. Rudolph, H. Görls, J. Talarmin, P. Schollhammer, M. El-khateeb and W. Weigand, *Organometallics*, 2013, **32**, 4523-4530.

25 B. C. Manor, M. R. Ringenberg and T. B. Rauchfuss, *Inorg. Chem.*, 2014, **53**, 7241-7247.

26 D. Zheng, N. Wang, M. Wang, S. Ding, C. Ma, M. Y. Darensbourg, M. B. Hall and L. Sun, *J. Am. Chem. Soc*., 2014, **136**, 16817-16823.

27 (a) L.-C. Song, J. Cheng, J. Yan, H.-T. Wang, X.-F. Liu and Q.-M. Hu, *Organometallics*, 2006, **25**, 1544-1547; (b) L.-C. Song, C.-G. Li, J. Gao, B.-S. Yin, X. Luo, X.-G. Zhang, H.-L. Bao and Q.-M. Hu, *Inorg. Chem*., 2008, **47**, 4545-4553; (c) L.-C. Song, C.-G. Li, J.-H. Ge, Z.-Y. Yang, H.-T. Wang, J. Zhang and Q.-M. Hu, *J. Inorg. Biochem.*, 2008, **102**, 1973-1979 ; (d) L.-C. Song, M.-Y. Tang, F.-H. Su and Q. -M. Hu, *Angew. Chem. Int. Ed*., 2006, **45**, 1130-1133.

28 (a) L.-C. Song, J.-H. Ge, X. -G. Zhang, Y. Liu and Q.-M. Hu, *Eur. J. Inorg. Chem*., 2006, 3204-3210; (b) L.-C. Song, M.-Y. Tang, S.-Z. Mei, J.-H. Huang and Q.-M. Hu, *Organometallics*, 2007, **26**, 1575-1577; (c) L.-C. Song, H.-T. Wang, J.-H. Ge, S.-Z. Mei, J. Gao, L.-X. Wang, B. Gai, L.-Q. Zhao, J. Yan and Y.-Z. Wang,

Organometallics, 2008, **27**, 1409-1416; (d) L.-C. Song, L.-X. Wang, B.-S. Yin, Y.-L. Li, X.-G. Zhang, Y.-W. Zhang, X. Luo and Q.-M. Hu, *Eur. J. Inorg. Chem.*, 2008, 291-297.

29 (a) L.-C. Song, J.-H. Ge, J. Yan, H.-T. Wang, X. Luo and Q.-M. Hu, *Eur. J. Inorg. Chem.*, 2008, 164-171; (b) L.-C. Song, Z.-Y. Yang, H.-Z. Bian, Y. Liu, H.-T. Wang, X.-F. Liu and Q.-M. Hu, *Organometallics*, 2005, **24**, 6126-6135; (c) L.-C. Song, B. Gai, H.-T. Wang and Q.-M. Hu, *J. Inorg. Biochem.*, 2009, **103**, 805-812; (d) W. Gao, L.-C. Song, B.-S. Yin, H.-N. Zan, D.-F. Wang and H.-B. Song, *Organometallics*, 2011, **30**, 4097-4107; (e) L.-C. Song, W. Gao, X. Luo, Z.-X. Wang, X.-J. Sun and H.-B. Song, *Organometallic,* 2012, **31**, 3324-3332; (f) L.-C. Song, B. Gai, Z.-H. Feng, Z.-Q. Du, Z.-J. Xie, X.-J. Sun and H.-B. Song, *Organometallics*, 2013, **32**, 3673-3684; (g) L.-C. Song, M. Cao, Z.-Q. Du, Z.-H. Feng, Z. Ma and H.-B. Song, *Eur. J. Inorg. Chem.*, 2014, 1886-1895.

30 M. W. W. Adams, L. E. Mortenson and J.-S. Chen, *Biochim. Biophys. Acta*, 1981, **594**, 105-176.

31 N. Wang, M. Wang, L. Chen and L. Sun, *Dalton Trans.*, 2013, **42**, 12059-12071.

32 S. Tschierlei, S. Ott and R. Lomoth, *Energy Environ. Sci.*, 2011, **4**, 2340-2352.

33 X. Zhao, I. P. Georgakaki, M. L. Miller, J. C. Yarbrough and M. Y. Darensbourg, *J. Am. Chem. Soc.*, 2001, **123**, 9710-9711.

34 J. A. Wright and C. J. Pickett, *Chem. Commun.*, 2009, 5719-5721.

35 A. Jablonskytė, J. A. Wright and C. J. Pickett, *Eur. J. Inorg. Chem.*, 2011, 1033-1037.

36 J. A. Wright, L. Webster, A. Jablonskytė, P. M. Woi, S. K. Ibrahim and C. J. Pickett, *Faraday Discuss*, 2011, **148**, 359-371.

37 X. Zhao, C.-Y. Chiang, M. L. Miller, M. V. Rampersad and M. Y. Darensbourg, *J. Am. Chem. Soc.*, 2003, **125**, 518-524.

38 L.-C. Song, Z.-Y. Yang, Y.-J. Hua, H.-T. Wang, Y. Liu and Q.-M. Hu, *Organometallics*, 2007, **26**, 2106-2110.

39 L.-C. Song, Q.-S. Li, Z.-Y. Yang, Y.-J. Hua, H.-Z. Bian and Q.-M. Hu, *Eur. J. Inorg. Chem.*, 2010, 1119-1228.

40 X. Zhao, I. P. Georgakaki, M. L. Miller, R. Mejia-Rodriguez, C.-Y. Chiang and M. Y. Darensbourg, *Inorg. Chem*., 2002, **41**, 3917-3928.

41 J. L. Nehring and D. M. Heinekey, *Inorg. Chem.*, 2003, **42**, 4288-4292.

42 A. Jablonskytė, J. A. Wright and C. J. Pickett, *Dalton Trans.*, 2010, **39**, 3026-3034.

43 S. E. Doris, J. J. Lynch, C. Li, A. W. Wills, J. J. Urban and B. A. Helms, *J. Am. Chem. Soc*., 2014, **136**, 15702-15710.

44 Y. Nicolet, A. L. de Lacey, X. Vernède, V. M. Fernandez, E. C. Hatchikian and J. C. Fontecilla-Camps, *J. Am. Chem. Soc*., 2001, **123**, 1596- 1601.

45 D. Sellmann, F. Geipel and M. Moll, *Angew. Chem. Int. Ed.*, 2000, **39**, 561-563.

46 J. P. Collman, P. S. Wagenknecht, R. T. Hembre and N. S. Lewis, *J. Am. Chem. Soc.*, 1990, **112**, 1294-1295.

47 A. C. Albeniz, D. M. Heinekey and R. H. Crabtree, *Inorg. Chem*., 1991, **30**, 3632-3635.

48 W. Wang, M. J. Nilges, T. B. Rauchfuss and M. Stein, *J. Am. Chem. Soc*., 2013, **135**, 3633-3639.

49 *CrystalClear and CrystalStructure*, Rigaku and Rigaku Americas, The Woodlands, TX, **2007**.

50 Sheldrick, G. M. *SHELXS-97, Program for solution of crystal structures*, University of Göttingen, Germany, **1997**.

51 Sheldrick, G. M. *SHELXS-97, Program for refinement of crystal structures*, University of Göttingen, Germany, **1997**.

The Graphical Contents Entry

Synthesis, characterization, and H/D exchange of μ-hydride-containing [FeFe]-hydrogenase subsite models formed by protonation reactions of (μ-TDT)$Fe_2(CO)_4(PMe_3)_2$ (TDT = SCH_2SCH_2S) with protic acids

Li-Cheng Song,* An-Guo Zhu, and Yuan-Qiang Guo

The first TDT ligand-containing μ-hydride models for [FeFe]-hydrogenases (**2–7**) have been prepared and the H/D exchange reactions of **7** with deuterium reagents such as D_2, D_2O, and DCl are studied, for example: